Time-resolved Quantitative Proteome Analysis of *In Vivo* Intestinal Development[S]

Jenny Hansson‡§‖, Alexandre Panchaud§, Laurent Favre¶, Nabil Bosco¶, Robert Mansourian§, Jalil Benyacoub¶, Stephanie Blum¶, Ole N. Jensen‡, and Martin Kussmann§

Postnatal intestinal development is a very dynamic process characterized by substantial morphological changes that coincide with functional adaption to the nutritional change from a diet rich in fat (milk) to a diet rich in carbohydrates on from weaning. Time-resolved studies of intestinal development have so far been limited to investigation at the transcription level or to single or few proteins at a time. In the present study, we elucidate proteomic changes of primary intestinal epithelial cells from jejunum during early suckling (1–7 days of age), middle suckling (7–14 days), and weaning period (14–35 days) in mice, using a label-free proteomics approach. We show differential expression of 520 proteins during intestinal development and a pronounced change of the proteome during the middle suckling period and weaning. Proteins involved in several metabolic processes were found differentially expressed along the development. The temporal expression profiles of enzymes of the glycolysis were found to correlate with the increase in carbohydrate uptake at weaning, whereas the abundance changes of proteins involved in fatty acid metabolism as well as lactose metabolism indicated a nondiet driven preparation for the nutritional change at weaning. Further, we report the developmental abundance changes of proteins playing a vital role in the neonatal acquisition of passive immunity. In addition, different isoforms of several proteins were quantified, which may contribute to a better understanding of the roles of the specific isoforms in the small intestine. In summary, we provide a first, time-resolved proteome profile of intestinal epithelial cells along postnatal intestinal development. ***Molecular & Cellular Proteomics 10: 10.1074/mcp.M110.005231, 1–12, 2011.***

The postnatal development of the gastrointestinal tract is a very dynamic process, including an intensive growth together with a complex process of differentiation. The most profound changes are observed in the epithelium of the small intestine. Developmental adaption of small intestinal enterocytes is considered to be preprogrammed, but several studies have suggested that external stimuli, such as microbial colonization and diet, may modulate the timing of age-related changes during early postnatal life (1–5). The joint action of environmental and intrinsic stimuli may therefore be responsible for initiating the adaptive changes and influence the precise timing and the level of expression of specific intestinal markers.

Perinatal development of the small intestine can be divided into three phases: the prenatal, the neonatal, and the postweaning phase. In late fetal life, long and thin villi shape the small intestinal epithelium, and the enterocytes (the main absorptive cells of the intestine) are characterized by their apical microvilli (6). Dividing cells populate the flat intervillous region, whereas differentiated cells migrate up the villus. Before birth in humans and during the first week of age in mice, crypts develop from the intervillous region, resulting in the formation of a distinct proliferating compartment (6). Final intestinal development in the postweaning phase is characterized by growth of crypts and villi, which results in an expansion of the villi from a finger-like to a leaflike shape (7). Furthermore, a faster replacement of enterocytes along the villus is observed, to reach the adult turnover rates estimated to be around 3 days in mice (6, 8).

Between the three mentioned phases of intestinal development, two abrupt changes in diet occur: at birth, when the intestine switches from processing dilute amniotic fluid to digesting milk; and at weaning, when the adaption to solid food begins. During suckling, the main energy source is fatty acids, whereas the principal source of energy after weaning is supplied by complex carbohydrates. Several enzymes expressed by enterocytes and responsible for nutrient digestion (*e.g.* lactase, sucrase, maltase, and aminopeptidase) are known to change in activity during postnatal development (9). Furthermore, enterocytes of fetal humans and suckling rodents possess a unique feature in the presence of large vacuoles, important for amniotic and colostral macromolecule transport, such as the transport of immunoglobulins (10, 11).

Starting at birth, the mammalian intestinal tract is rapidly colonized by bacteria from the mother and the surrounding environment, eventually resulting in a dense and diverse in-

From the ‡Department of Biochemistry and Molecular Biology, University of Southern Denmark, Campusvej 55, 5230 Odense M, Denmark, §Department of Bioanalytical Science, Nestlé Research Center, Vers-chez-les-Blanc, P.O. Box 44, 1000 Lausanne 26, Switzerland, ¶Department of Nutrition and Health, Nestlé Research Center, Vers-chez-les-Blanc, P.O. Box 44, 1000 Lausanne 26, Switzerland

Received September 29, 2010, and in revised form, December 20, 2010

Published, MCP Papers in Press, December 29, 2010, DOI 10.1074/mcp.M110.005231

testinal microbiota. The changes of the mammalian intestinal ecosystem are influenced by the diet and profound changes occur at weaning, with a change from dominance of facultative anaerobes to obligate anaerobes (12, 13). It is well documented that microbiota composition as well as its metabolic activity strongly influences gut physiology and overall health condition (14, 15). In that respect, growing evidence supports that microbiota drive key postnatal developmental events in the gut, and specific bacteria have, for example, been shown to influence fatty acid metabolism (1, 3).

Studies of intestinal development over time have so far been limited to investigation at the transcription level or targeted nonproteomic analysis of single or few proteins (4, 5, 16–21). Recently, a study using microarray analysis examined gene expression changes in jejunum of rats during the transient suckling-weaning period, demonstrating the up-regulation of many genes involved in digestion, absorption, excretion, and transcription during this period (21). However, although the mentioned studies are based on whole-tissue samplings of the small intestine, analyses of primary intestinal epithelial cells (IECs) lag behind.

In the present study, we monitor proteomic changes of primary IECs during early suckling, middle suckling, and weaning period in mice, using a label-free quantitative proteomics approach. The temporal expression pattern of a multitude of proteins is described and compared with previous findings at transcription level and across different species. In conclusion, we provide a first, time-resolved proteome profile of intestinal epithelial cells along postnatal intestinal development.

EXPERIMENTAL PROCEDURES

The study was performed according to the guidelines of the Swiss regulations of animal welfare and was approved by the Veterinary Office of Canton de Vaud (Switzerland).

Chemicals—Dithiotreitol (DTT), iodoacetamide, EDTA, ammonium bicarbonate, formic acid, trifluoroacetic acid, Percoll, calcium- and magnesium-free Hank's balanced salt solution (HBSS), phosphate-buffered saline, liquid chromatography (LC)-MS grade water and acetonitrile (ACN) were purchased from Sigma-Aldrich (St.Louis, MO). RapiGest was purchased from Waters (Milford, MA). Sequencing-grade modified trypsin was obtained from Promega (Madison, WI). PE anti-mouse EpCAM and APC anti-mouse CD45 was purchased from eBioscience (San Diego, CA). Bicinchoninic acid (BCA)[1] protein assay kit was purchased from Pierce (Rockford, IL). Fetal calf serum (FCS) was purchased from Bioconcept (Allschwill, Switzerland).

Isolation of Intestinal Epithelial Cells (IECs) —Mouse pups were delivered from six pregnant C57BL/6J mice (purchased from Charles River, France) and maintained with their mothers until weaning at 21 days (D). At 1 D, 7 D, 14 D, and 35 D, one mouse per litter (3 females, 3 males) was sacrificed by cervical dislocation and intestinal epithelial cells were isolated as described previously (22, 23), with slight modifications. Briefly, the jejunum was dissected and fat and Peyer's patches were removed. The tissue was cut longitudinally and rinsed by gentle shaking in ice-cold HBSS containing 5% heat-inactivated FCS (washing buffer). The supernatant was removed and fresh washing buffer was added. This was repeated (at least four times) until the supernatant remained clear. The tissue was then cut into 1-cm lengths and placed in HBSS containing 10% FCS, 1 mM EDTA, 1 mM DTT, 100 units/ml penicillin, and 100 μg/ml streptomycin (dissociation buffer). After incubation with gentle shaking for 20 min at 37 °C, the supernatant was recovered and placed on ice. The tissue was again placed in dissociation buffer and the procedure repeated once. The supernatants were filtered through a 100 μm cell strainer and cells were washed in HBSS by two centrifugations at 300 g for 7 min. Finally, the primary IECs were purified by centrifugation through a 25/40% discontinuous Percoll gradient at 600 $\times$ *g* for 20 min. Primary IECs were collected from the interface and washed in PBS. Assessed by flow cytometry, purity of isolated cells was routinely >95% EpCAM+ and <0.5% CD43+.

Protein Extraction and Digestion—Cells were lysed with 0.1% RapiGest in 100 mM ammonium bicarbonate at 4 °C for 30 min. Cell debris were removed by centrifugation and the total protein concentration of each cell lysate was measured by BCA according to the manufacturer's instructions. After reduction of disulfide bonds with 5 mM DTT for 30 min at 50 °C and alkylation of cysteines with 10 mM iodoacetamide for 60 min at room temperature in the dark, the proteins were digested overnight with trypsin (1:50 (w/w) trypsin:protein ratio) at 37 °C. The reaction was stopped by adding trifluoroacetic acid to a final concentration of 0.5% (v/v) and RapiGest was precipitated by further incubation at 37 °C for 30 min. Following centrifugation the supernatants were collected and protein digests were stored at −20 °C until further use.

Liquid Chromatography Electrospray Ionization Tandem MS (LC-ESI-MS/MS) Analysis—Protein digests were analyzed in duplicate using a LC-ESI-MS/MS system consisting of a Rheos Allegro pump (Thermo Fisher Scientific, Waltham, MA), a PAL HTC autosampler (CTC Analytics, Zwingen, Switzerland), and an LTQ-XL Orbitrap mass spectrometer (Thermo Fisher Scientific, Waltham, MA) equipped with a nano-ESI source from the same supplier. The mobile phases for LC separation were 0.1% (v/v) formic acid, 2% (v/v) ACN in LC-MS grade water (solvent A) and 0.1% (v/v) formic acid, 80% (v/v) ACN in LC-MS grade water (solvent B). Using the information from the BCA assay, 750 ng protein digest was first loaded and desalted on a homemade precolumn (Magic C18AQ 5 μm 200 Å (Michrom Bioresources, Auburn, CA), IntegraFrit™ 100 μm $\times$ 30 mm (New Objective, Woburn, MA)) at 2 μl/min with solvent A for 10 min. The valve was then switched to connect the trap column with a homemade analytical column (Magic C18AQ 3 μm 200 Å (Michrom Bioresources, Auburn, CA), TSP fused silica tubing 75 μm $\times$ 150 mm (BGB Analytik, Switzerland)) directly installed in the nanoESI interface of the MS. Peptides were separated at a flow rate of 300 nl/min with a linear gradient from 5 to 70% solvent B in 60 min.

The nanoESI source operated in positive-ion mode at 1.8 kV with a capillary temperature of 200 °C. Full scan spectra from *m/z* 350 to 2000 at resolution 60,000 (profile mode) were acquired in the Orbitrap MS and in parallel five data-dependent MS/MS spectra of most intense ions were acquired in the LTQ-XL ion trap using collision induced dissociation with a normalized collision energy setting of 35. The lock mass option was activated and the background signals with the masses 391.284286 and 445.120024 were used as lock masses. Dynamic exclusion was employed for 30 s. The data associated with this manuscript may be downloaded from ProteomeCommons.org Tranche using the following hash: HIbd/oz/9Fp7ETfju8F2/b+cRLMVsJXZnEo+fT8/umfF4bs5+HwY6SzuO3H9)WJmOEj8X+A7Jp5Dd9l5zS6hheVuCloAAAAAAAAYxw==.

Identification and Label-free Quantification of Proteins—Protein quantification was done by processing the acquired LC-MS data with

[1] The abbreviations used are: BCA, bicinchoninic acid; CC, correlation coefficient; D, Day(s); FABP, fatty acid binding protein; FC, fold change; GO, Gene Ontology; HBSS, Hank's balanced salt solution; IEC, intestinal epithelial cell.

the software Progenesis LC-MS (version 2.6, Nonlinear Dynamics, Newcastle, UK), as described here. The 48 LC-MS runs were aligned based on paired feature detection (150 vectors on each two-dimensional map (*m/z versus* retention time)), using one LC-MS run as reference. Normalization was based on the assumption that some proteins (and therefore peptide ions) will not be changing in abundance in the experiment. For each feature within the robust estimation limits, a quantitative abundance ratio between the run being normalized and the reference run was calculated. Using these abundance ratios, the normalization factor was calculated with a recursive median approach. MS/MS spectra from features with charge +2, +3 and +4 were exported and searched against the SwissProt database (release 2010_06, taxonomy Mus: 16,302 entries) using Mascot (version 2.3, Matrix Science, London, UK). The following Mascot search parameters were used: enzyme trypsin with two missed cleavages were allowed, fixed modification used was carbamidomethyl (C), variable modifications used were deamidated (NQ) and oxidation (M), peptide mass tolerance was set to 5 ppm and fragment ion mass tolerance was set to 1 Da. The peptide ion score cutoff was set to allow a 2% false discovery rate, as estimated by a search against a decoy database. Peptide identifications assigned to more than one protein were then removed to avoid errors in the quantification and only proteins with ≥2 peptides were kept for statistical analysis. Within the Progenesis LC-MS software, peptide abundance values were calculated as the sum of the peak areas within the isotope boundaries of the feature. Protein abundance values were calculated as the sum of the abundance values of all peptides belonging to the protein.

Statistical Analysis—Protein abundance values were exported from Progenesis LC-MS software and the dataset was transformed with the arcsinh (inverse hyperbolic sine) function within Excel in order to reach a normal distribution of the data and thereby allow for the statistical analysis. Using Partek software (St. Louis, MO), the statistical analysis was performed with a nested ANOVA, in order to consider the hierarchy in the data arising from including both biological and technical replicates, and thereby accounting for the different variance contribution of each of the two factors. In order to attribute a certain expression profile to each individual protein, differential expression of a protein was declared when the relative abundance differed between groups by $p < 0.05$. A protein was reported to be higher or lower expressed when its expression was respectively higher (fold change (FC) >1) or lower (FC < −1) at a later time point than at an earlier time point.

Protein Classification With Gene Ontology (GO)—To provide insight into the subcellular location of the identified proteins, proteins were annotated based on GO cellular components assignments by FatiGO (24). Differentially expressed proteins were mapped according to Panther classification of biological processes (25) by the web tool DAVID (Database for Annotation, Visualization and Integrated Discovery) (26, 27).

RESULTS AND DISCUSSION

Establishment of Label-free Quantitative Proteomics of Intestinal Development—The goal of this study was to elucidate proteomic changes of IECs along postnatal maturation of the murine intestine. We approached this with a label-free, quantitative proteomics method using four time-points along postnatal maturation to analyze the changes occurring at the three periods of early suckling (1–7 D), middle suckling (7–14 D), and weaning period (14–35 D) (Fig. 1). Note that weaning occurs at 21 D and the period from 14 D to 35 D therefore covers the preweaning to postweaning phase, but we refer to it as the weaning period throughout this manuscript. Because differences in protein expression have been shown along the crypt-villus axis (28) as well as in gene expression along the duodenal to ileal axis (16, 18), maximal homogeneity of the cells for protein extraction was of high importance. We therefore focused on purified isolations of primary enterocytes from jejunum, because the absorption and the final stages of digestion of the majority of nutrients take place in jejunum. We analyzed the whole cell lysates on a high mass resolution LTQ-Orbitrap instrument, in six biological and two technical replicates. Alignment of LC-MS runs, feature extraction, normalization, and calculation of protein abundance was performed with the Progenesis LC-MS software. Statistical analysis was performed with a nested ANOVA, to take into account the hierarchical structure arising from the inclusion of both biological and technical replicates.

In total 52′524 features were examined, resulting in the identification of 591 proteins (≥2 unique peptides per protein) from 3′905 identified peptides. Approximately half of the proteins (46%) were identified with ≤4 peptides (supplemental Tables S1 and S2). Classification of the identified proteins into cellular components based on gene ontology annotations revealed a diverse range of subcellular locations, with highest percentage of proteins found in mitochondrion, organelle membrane, organelle envelope, nucleus, and cytoskeleton (Fig. 2).

To assess the reproducibility of quantifying intestinal epithelial cell proteome changes, correlation coefficient (CC) was calculated for the protein abundance values between all replicated LC-MS runs. Average CC (±standard deviation) values were 0.948 ± 0.05, 0.976 ± 0.02, 0.930 ± 0.06, and 0.894 ± 0.06 at 1 D, 7 D, 14 D, and 35 D, respectively, indicating good technical reproducibility (supplemental Table S3). CC calculated from the average protein abundance obtained from the six biological replicates showed that the biological variability was greatest at 14 D (average ± standard deviation at 1 D, 7 D, 14 D, and 35 D was: 0.965 ± 0.01; 0.925 ± 0.07; 0.846 ± 0.12, and 0.910 ± 0.03, respectively).

Epithelial Cell Proteome Changes Along Intestinal Development—Analyzing the changes in protein abundance at the three periods of early suckling, middle suckling, and weaning period revealed a striking change of the proteome along intestinal maturation. 520 proteins (88%) were found to be differentially expressed ($p < 0.05$) during at least one of the three periods evaluated (supplemental Table S1), demonstrating the profound change in the physiology of epithelial cells along intestinal development. In early suckling period, between 1 D and 7 D, 98 proteins were found differentially expressed, whereas a remarkably greater difference was observed in the middle suckling period (7–14 D) and weaning (14–35 D), with 386 and 319 proteins differentially expressed, respectively. Although the down-regulation and up-regulation was relatively balanced in the early suckling period as well as in the weaning period, a much higher number of proteins showed a decrease in expression compared with increase in

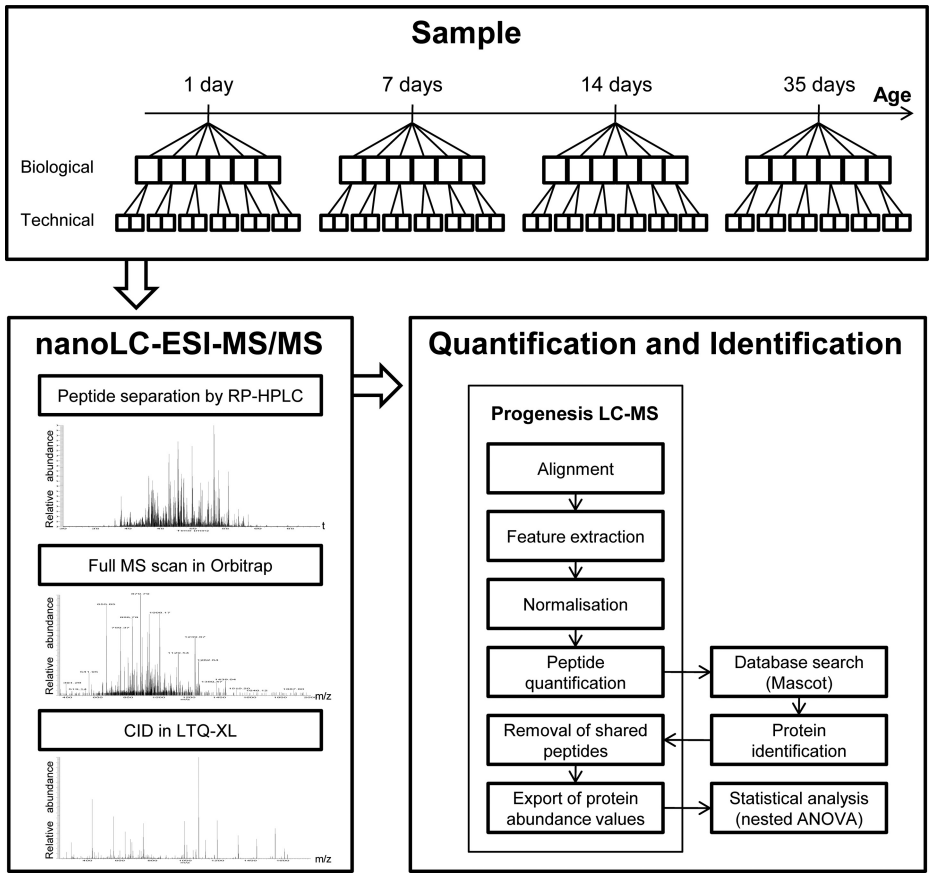

FIG. 1. **Flowchart of the label-free quantification approach.** Protein digests of lysates of IECs were prepared from six mice per time point and analyzed in duplicate on the LTQ-Orbitrap, as described in the Experimental Procedures. Raw data sets were processed by the quantification software Progenesis LC-MS. Protein identification was enabled with a Mascot database search. Protein abundance values were exported and statistical analysis was performed to identify differentially expressed proteins.

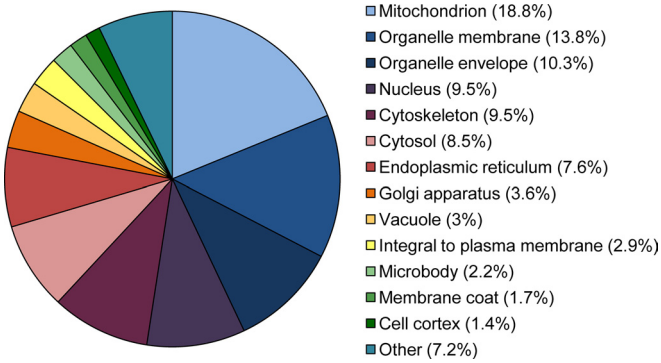

FIG. 2. **Percentage distribution of cellular components covered by GO annotations of all 591 identified proteins**.

the middle-suckling period (Fig. 3). These pronounced proteome changes in the later developmental stages, illustrate that the major change in function of the cells occurs after the first postnatal week.

Mapping of the data set to biological processes—To provide insight into which biological processes and pathways were the most affected during the course of intestinal maturation, the differentially expressed proteins were mapped according to Panther classification of biological processes. As expected considering the main role of intestinal epithelial cells to absorb and digest nutrients, differentially expressed proteins were highly involved in several metabolic processes, such as carbohydrate, fatty acid, and amino acid metabolism, *i.e.* overall in macronutrient metabolism (Fig. 4, supplemental Table S4). Furthermore, highly affected cellular processes included cell structure, reflecting the known morphological changes during the postnatal period and thereby further validating the approach.

Time-resolved Abundance Changes of Proteins Involved in Context-relevant Biological Processes—Next, the temporal expression patterns of individual proteins attributed to context-relevant biological processes were evaluated, in order to get a deeper insight into the changes of key processes of intestinal development.

Carbohydrate Metabolism—Among the differentially expressed proteins were 69 with a role in carbohydrate metabolism. Most of these showed the lowest expression at 2 weeks of age and many an elevated expression after weaning (Figs. 4 and 5, supplemental Table S4). The sodium-glucose cotransporter 1, which allows the cell to take up glucose and

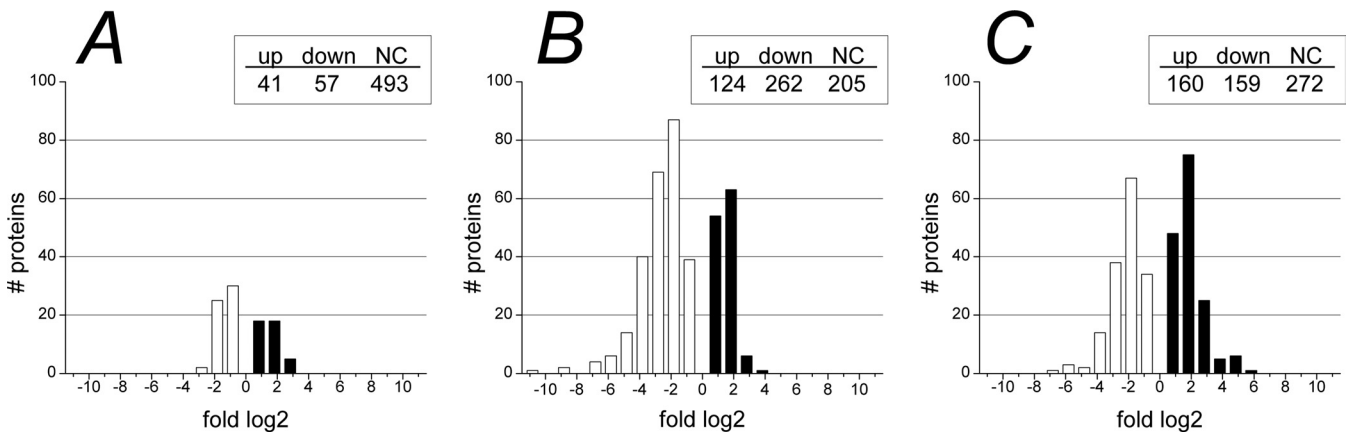

FIG. 3. **Distribution of fold changes of differentially expressed proteins during early suckling, middle suckling, and weaning period.** Distribution of fold changes are depicted for up- (*black*) and down- (*white*) regulated proteins ($p < 0.05$) during *A*, early suckling (1–7 D), *B*, middle suckling (7–14 D), and *C*, weaning (14–35 D) period. Fold changes are shown on a log2 scale. Total number of proteins with up-regulated, down-regulated, and no change (NC) in expression are shown in the inserted tables. Changes during early suckling (*A*) were subtle, whereas a remarkable greater difference occurred in the middle suckling period (*B*) and weaning period (*C*), with a high proportion of down-regulated proteins in the middle suckling period.

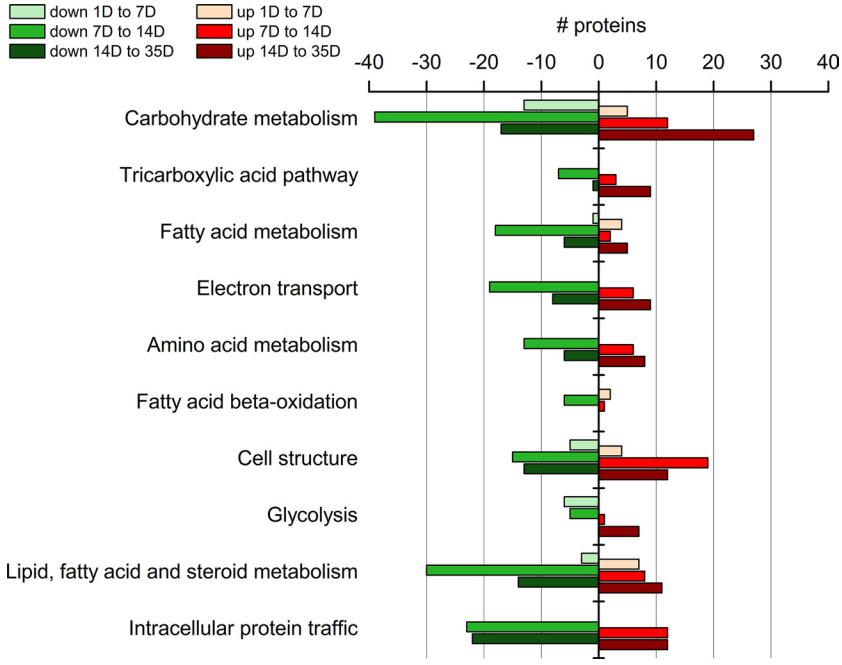

FIG. 4. **Top ten biological processes influenced during intestinal development.** Proteins with a significant ($p < 0.05$) change of expression along maturation were mapped onto biological processes according to Panther classification system. The presented top ten biological processes are sorted according to the *p* value after Bonferroni correction, which ranged between 1.0E-19 to 0.03. Within each biological process, number of proteins with a higher (red) and lower (green) expression along development are shown, with light color for proteins differentially expressed between 1 D and 7 D, middle shade between 7 D and 14 D, and dark color between 14 D and 35 D. The whole protein list is found in supplemental Table S4.

galactose by cotransport with sodium, was on the contrary temporarily elevated (threefold) during the middle suckling period, followed by a decrease to the original level of expression after weaning (Table I).

As part of carbohydrate metabolism, many enzymes involved in the glycolysis were coordinately down-regulated during the period of suckling, and up-regulated after weaning, correlating with the increase in carbohydrate uptake. These enzymes include glucose-6-phosphate isomerase, fructose-bisphosphate aldolase, triosephosphate isomerase, glyceraldehyde-3-phosphate dehydrogenase, phosphoglycerate kinase, phosphoglycerate mutase, enolase, and pyruvate kinase (Fig. 6, supplemental Table S4). Two isozymes of pyruvate kinase, the enzyme catalyzing the final step of the glycolysis, were identified (R/L and M1/M2) and showed different expression profiles. Pyruvate kinase M1/M2 showed a strong profile with a 1.7-fold decline from 1 D to 7 D, a further 1.3-fold decrease from 7 D to 14 D followed by a 6.5-fold increase from 14 D to reach maximal expression at 35 D. Isozyme R/L conversely showed an elevated expression already from 7 D (supplemental Table S1). Deduced from the expression profile of both pyruvate kinase isozymes, it appears possible that they exert different physical and kinetic properties also in intestinal epithelial cells, as for tumor cells for which the isozyme switch to M2 is known to be associated with the increased glycolytic metabolism that is characteristic of these cells (29).

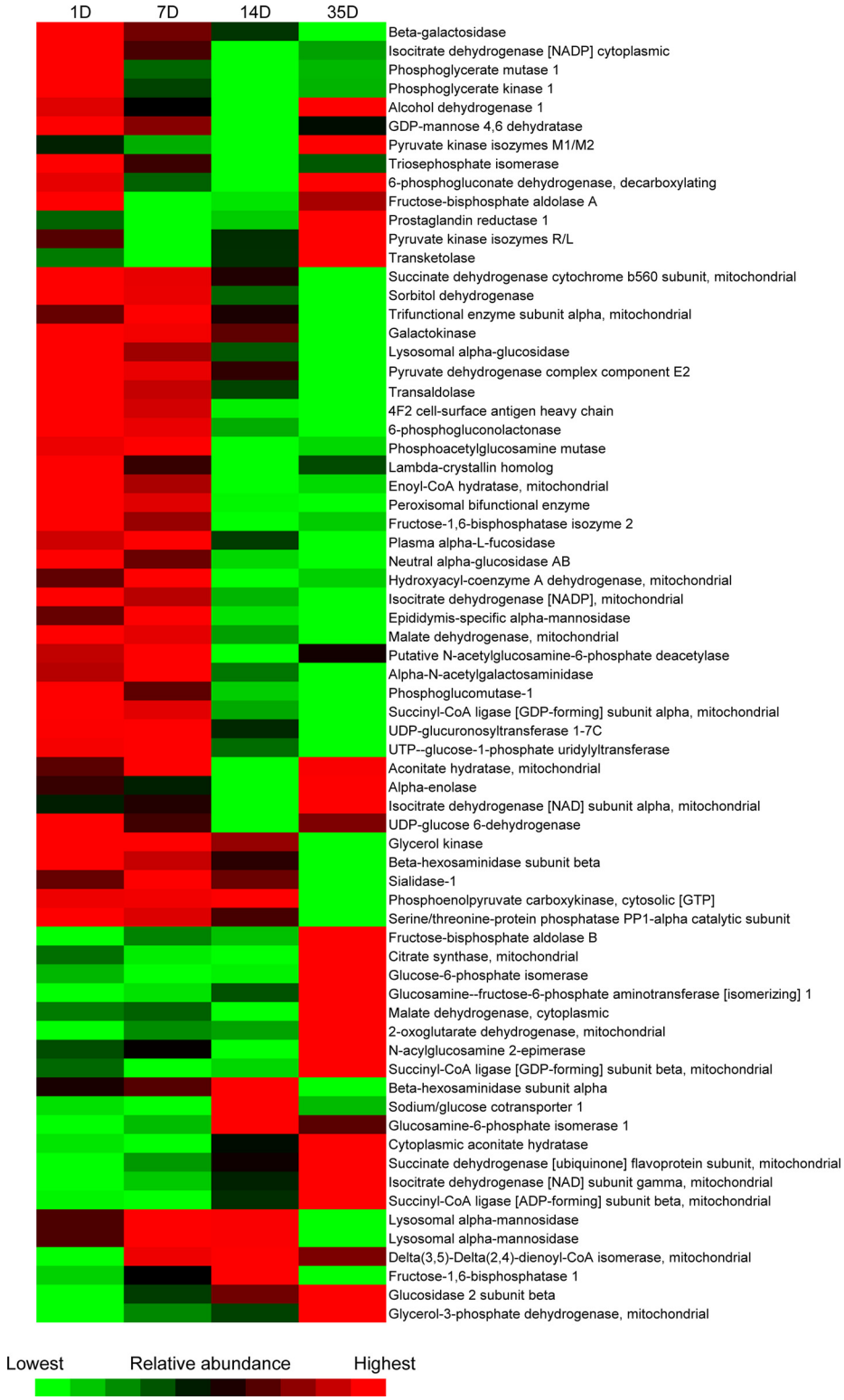

FIG. 5. **Abundance changes of proteins of carbohydrate metabolism during postnatal intestinal development.** For each protein, abundance is represented in a gradual color scale from lowest abundance (*bright green*) to highest abundance (*bright red*). Most proteins showed a reduced expression during suckling (1–14 D) and many increased in abundance at weaning (14–35 D). The respective fold changes for each protein are listed in supplemental Table S4.

A particularly important metabolic process during the suckling period is lactose metabolism, because the main carbohydrate source in milk is lactose. Attenuated expression along the maturation was observed for proteins involved in lactose metabolism (Table I). We identified β-galactosidase (lactase), which is bound to the apical membrane of enterocytes and hydrolyzes lactose to form glucose and galactose that further on can be absorbed by the enterocytes. In previously reported

TABLE I

Protein abundance changes of selected proteins along intestinal development

The protein fold changes (from early time-point to later time-point) including S.D. and *p* values are given for selected proteins, in the order of being mentioned in the text.

UniProt ID	Protein name	Peptides quantified	1 D to 7 D		7 D to 14 D		14 D to 35 D	
			fold change	*p* value	fold change	*p* value	fold change	*p* value
SC5A1_MOUSE	Sodium/glucose cotransporter 1	2	−1.08 ± 0.62	0.799	3.73 ± 0.62	2E-04	−3.13 ± 0.62	0.001
BGAL_MOUSE	Beta-galactosidase	9	−1.93 ± 0.38	0.002	−2.17 ± 0.38	4E-04	−2.57 ± 0.38	5E-05
GALK1_MOUSE	Galactokinase	3	−1.10 ± 0.65	0.767	−3.23 ± 0.65	0.001	−15.44 ± 0.65	3E-08
PGM1_MOUSE	Phosphoglucomutase-1	6	−1.64 ± 0.53	0.065	−2.54 ± 0.53	0.002	−1.16 ± 0.53	0.558
S27A4_MOUSE	Long-chain fatty acid transport protein 4	2	−1.11 ± 0.68	0.752	1.40 ± 0.68	0.317	2.24 ± 0.68	0.023
CD36_MOUSE	Platelet glycoprotein 4	2	−1.10 ± 0.43	0.647	−1.04 ± 0.43	0.838	−1.83 ± 0.43	0.009
FABPI_MOUSE	Fatty acid-binding protein, intestinal	2	−1.12 ± 0.70	0.743	−6.61 ± 0.70	2E-05	−8.39 ± 0.70	3E-06
FABPL_MOUSE	Fatty acid-binding protein, liver	10	−1.36 ± 0.44	0.166	1.20 ± 0.44	0.411	−1.40 ± 0.44	0.13
MOGT2_MOUSE	2-acylglycerol O-acyltransferase 2	4	−1.59 ± 1.05	0.371	−14.67 ± 1.05	3E-05	1.09 ± 1.05	0.862
MTP_MOUSE	Microsomal triglyceride transfer protein large subunit	31	1.03 ± 0.58	0.905	−4.39 ± 0.58	3E-05	−1.97 ± 0.58	0.024
APOA4_MOUSE	Apolipoprotein A-IV	10	1.13 ± 0.36	0.479	1.29 ± 0.36	0.158	−1.15 ± 0.36	0.418
AMPN_MOUSE	Aminopeptidase N	12	−1.04 ± 0.52	0.865	−1.08 ± 0.52	0.753	−2.38 ± 0.52	0.002
NALDL_MOUSE	N-acetylated-alpha-linked acidic dipeptidase-like protein	2	−1.74 ± 1.96	0.563	3.84 ± 1.96	0.168	−43.30 ± 1.96	7E-04
AMPE_MOUSE	Glutamyl aminopeptidase	5	−1.64 ± 0.35	0.009	1.03 ± 0.35	0.872	−2.22 ± 0.35	1E-04
DPP2_MOUSE	Dipeptidyl peptidase 2	3	−2.10 ± 0.80	0.067	−5.62 ± 0.80	2E-04	1.14 ± 0.80	0.738
PEPD_MOUSE	Xaa-Pro dipeptidase	3	1.32 ± 0.35	0.109	1.65 ± 0.35	0.007	3.07 ± 0.35	2E-06
XPP1_MOUSE	Xaa-Pro aminopeptidase 1	8	−1.17 ± 0.45	0.465	−1.84 ± 0.45	0.011	2.10 ± 0.45	0.003
AMPB_MOUSE	Aminopeptidase B	4	−1.30 ± 0.50	0.294	1.75 ± 0.50	0.03	1.82 ± 0.50	0.021
AMPL_MOUSE	Cytosol aminopeptidase	8	1.03 ± 0.36	0.853	1.85 ± 0.36	0.002	1.30 ± 0.36	0.147
CNDP2_MOUSE	Cytosolic non-specific dipeptidase	10	−1.76 ± 0.30	9E-04	−1.30 ± 0.30	0.086	2.05 ± 0.30	8E-05
FCGRN_MOUSE	IgG receptor FcRn large subunit p51	4	3.00 ± 0.57	6E-04	−1.84 ± 0.57	0.037	−5.48 ± 0.57	4E-06
AEGP_MOUSE	Apical endosomal glycoprotein	13	−1.25 ± 0.31	0.153	−1.04 ± 0.31	0.812	−5.48 ± 0.31	4E-10
VILI_MOUSE	Villin-1	15	1.20 ± 0.17	0.033	1.31 ± 0.17	0.003	1.42 ± 0.17	2E-04
SPTB2_MOUSE	Spectrin beta chain, brain 1	6	−1.26 ± 0.32	0.141	1.38 ± 0.32	0.044	1.69 ± 0.32	0.002
FLNB_MOUSE	Filamin-B	7	−1.48 ± 0.48	0.108	3.60 ± 0.48	2E-05	3.39 ± 0.48	4E-05

10.1074/mcp.M110.005231–7

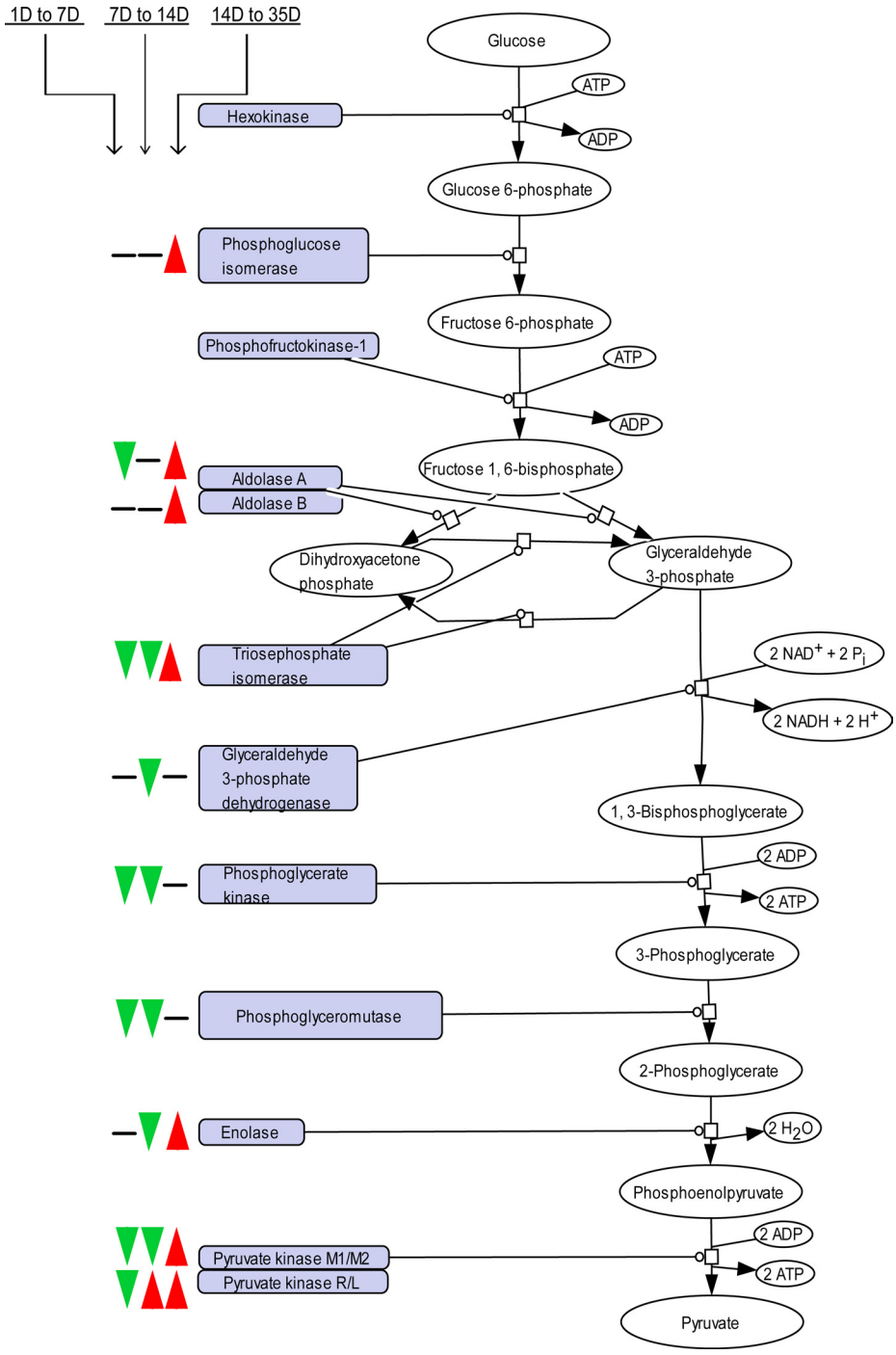

FIG. 6. **Time-resolved abundance changes of enzymes of the glycolysis during intestinal development.** The three signs from the left to the right depict the change of expression in the early suckling, middle suckling, and weaning period, respectively, with a *green arrow* or *red arrow* for decrease or increase in expression, respectively. Enzymes without signs were not identified. Proteins and respective fold changes are listed in supplemental Table S4.

studies, lactase mRNA levels and activity have been shown to be elevated soon after birth followed by a decrease during the suckling period (16, 18). We found a continuous decline in lactase expression from the first day of age, with more than a 10-fold decrease to the 35th day of age, indicating that lactose metabolism declines whereas the neonate is still suckling and has not yet encountered solid food. Furthermore, the expression of proteins related to galactose metabolism was also reduced during the course of maturation: during middle-suckling period, we observed reduced expression levels of galactokinase and phosphoglucomutase (3.2-fold and 2.5-fold, respectively) and a further strong reduction of galactokinase level during weaning (15.4-fold).

Lipid and Fatty Acid Absorption and Metabolism—Because fatty acids in milk are absorbed from the small intestine, proteins involved in fatty acid absorption and metabolism play a prominent role in development. Several proteins with a key role in dietary fat absorption in the small intestine were found

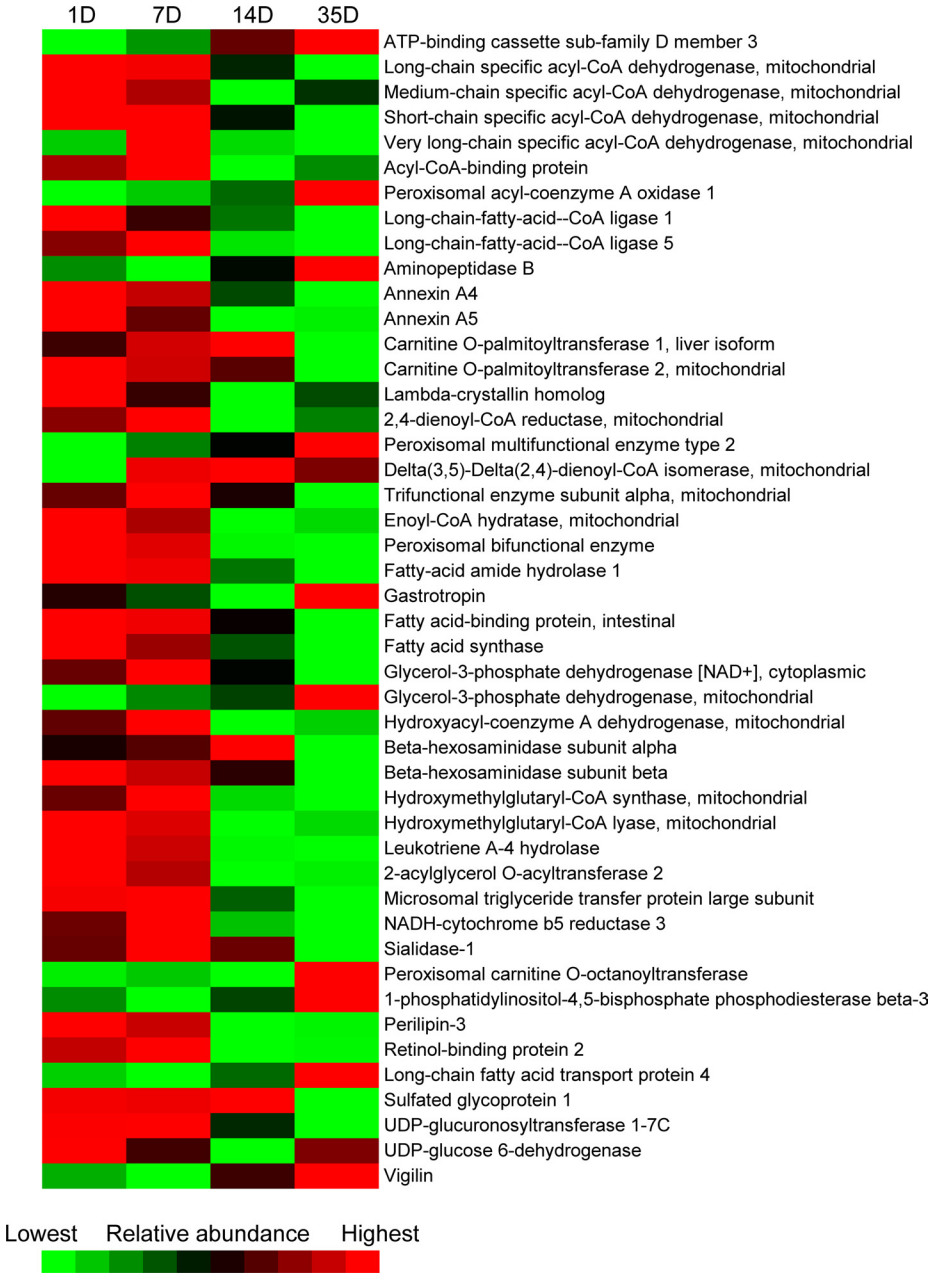

FIG. 7. **Abundance changes of proteins of lipid, fatty acid, and steroid metabolism during postnatal intestinal development.** For each protein, abundance is represented in a gradual color scale from lowest abundance (*bright green*) to highest abundance (*bright red*). A marked decrease in expression was found for most proteins during the middle-suckling period (7–14 D). The respective fold changes for each protein are listed in supplemental Table S4.

to be differentially expressed along the intestinal development. Most of these were found to have a profile of highest expression in the early suckling period and a pronounced decrease in the middle-suckling period, *i.e.* already before the switch from a fatty acid-rich diet to carbohydrate-rich diet (Figs. 4 and 7, supplemental Table S4). Examples of fatty acid metabolism proteins with a strongly reduced expression in the middle suckling period were peroxisomal bifunctional enzyme, 2-acylglycerol *O*-acyltransferase, medium-chain specific acyl-CoA dehydrogenase, enoyl-CoA hydratase, hydroxymethylglutaryl-CoA lyase and fatty-acid amide hydrolase (28-, 15-, 10-, 8-, 7-, and 6-fold, respectively). Together with the observed early decline of proteins involved in lactose metabolism, these results may represent the preprogrammed changes that occur to prepare for the nutritional change at weaning. However, although an intrinsic rather than a food-driven stimulus may be suggested to control the changes of expression of proteins involved in the mentioned metabolic processes, other external stimuli should also be considered. These include the composition of the microbiota as well as the development of the immune system, which through cross talk with the IECs may provide maturational signals (30). Supporting a role of microbiota, fatty acid metabolism in piglets has been shown to be influenced by the presence of specific bacteria (1). In addition, the fact that the nutrient composition of the milk itself changes along lactation must not be neglected (31).

Interestingly, two enzymes acting on the peroxisomal β-oxidation pathway for fatty acids, peroxisomal acyl-coenzyme A oxidase 1 (Acox1) and peroxisomal multifunctional enzyme type 2, were elevated throughout the course of maturation, with a sharp increase at weaning. In contrast to our results, the expression of the Acox1 corresponding gene has been shown to decline after weaning in rats (21). Such a difference is often seen between mRNA level and the final expression level of the protein, and may be because of post-transcriptional mechanisms controlling the mRNA translation and protein degradation rate (32, 33). Down-regulation of mRNA concurrent with up-regulation of protein expression, as in the case of Acox1, may, for example, occur when the half-life of a protein is increased because of stabilization and the accumulation of the protein acts as a repressor of transcription.

In the intestine, triacylglycerol (the dominant fat in diet) is digested into free fatty acids and monoacylglycerol before absorption by the enterocytes. There is some controversy whether fatty acids are taken up passively by diffusion or actively via specific transporters located in the apical plasma membrane of enterocytes (34). We identified two transporters presumed to be involved in intestinal fatty acid uptake: FATP4, which has been suggested to play a key role in the uptake of long-chain fatty acids and to be the principal fatty acid transporter in enterocytes (35); and platelet glycoprotein (CD36) (Table I). FATP4 was found to be up-regulated 2.2-fold after weaning, whereas CD36 was downregulated 1.8-fold, raising the possibility of different functional importance of the two transporters during the intestinal development. The up-regulation of FATP4 supports the argument of Tso *et al.* (34) that with a low concentration of fatty acids, they are taken up actively with transporters, whereas with a high concentration, the majority are taken up passively by the enterocytes.

Fatty acid-binding proteins (FABPs) are considered to be implicated in the transfer of absorbed fatty acids to the endoplasmic reticulum where the resynthesis of complex lipids takes place. The two major isoforms of FABP found in enterocytes, intestinal-type (I-FABP) and liver-type (L-FABP), are known to have different binding specificity and their mRNA levels have previously been studied in rats during postnatal intestinal development. I-FABP mRNA levels remain constant during the suckling period, whereas the mRNA levels of L-FABP gradually increase during the suckling period and then sharply declines at the end of weaning (17, 20). We identified both isoforms, which showed different expression profiles in comparison to the mentioned previous studies (Table I). We found a 6.6-fold down-regulation of I-FABP in the middle-suckling period and further 8.4-fold during weaning. We also saw that the protein expression of L-FABP is not significantly altered during maturation. These results again show that mRNA levels do not always reflect the relative protein abundances, as discussed above (32, 33). More importantly, the different expression profiles of I-FABP and L-FABP that we observe may be because of the influence of the microbial colonization, because the expression of the two isoforms has been shown to be mediated by specific bacteria in pigs (1).

Two proteins necessary for the assembly of lipoprotein in intestinal epithelial cells were identified: a marked decrease (15-fold) was observed in the middle-suckling period for the enzyme 2-acylglycerol *O*-acyltransferase 2, which catalyzes the resynthesis of triglycerides (Table I). This protein has previously been shown to be up-regulated in mice fed a high fat diet and its activity in liver to be higher during the suckling period than in the adult rat (36, 37). Microsomal triglyceride transfer protein, an enzyme that binds the resynthesized triacylglycerides and transfers them for binding to apolipoprotein, also showed a reduced expression between 7 D and 14 D (4.4-fold) and further from 14 D to 35 D (2.0-fold) (Table I). These results were in line with what has previously been shown in developing swine intestine, where the protein expression of microsomal triglyceride transfer protein decreased after weaning (19). The only apolipoprotein identified was apolipoprotein A-IV and it was not significantly differentially expressed during development.

Peptide Metabolism—Digestion of dietary proteins begins in the stomach, but the proteolysis in the small intestine also plays a major role. Peptidases are found in enterocytes both as integral membrane proteins and as cytosolic proteins. Their function is to cleave peptides into single amino acids or very small peptides. Several peptidases were identified and showed different expression profiles. Whereas cytoplasmic peptidases as well as one lysosomal peptidase showed both decreasing and increasing patterns, all three membrane bound peptidases identified were found to have a decreased expression during maturation (Table I). Aminopeptidase N, which is known to be highly expressed on the apical surface of enterocytes, was down-regulated 2.4-fold in the weaning period. The less characterized *N*-acetylated-α-linked acidic dipeptidase-like protein markedly decreased (43-fold) in the same period. Further, glutamyl aminopeptidase was found to decline in expression both in the early suckling period (1.6-fold) and after weaning (2.2-fold) (Table I). The data therefore suggests an importance of membrane bound peptidases during the early postnatal life.

Nonselective Uptake of Intact Proteins and Selective Uptake of IgG During Suckling—Enterocytes in proximal small intestine of suckling rodents direct active, receptor-mediated endocytosis and transcytosis of IgG from maternal milk, helping the newborn animals to acquire passive immunity (38, 39). This highly selective uptake of IgG is mediated by the neonatal Fc receptor (IgG receptor FcRn) at the apical surface of the epithelial cells. Our analysis identified the large subunit p51 of the FcRn and its expression was found to be elevated during the first 7 days of life (threefold from 1 D), then to diminish 1.8-fold in the middle suckling period and to further decline 5.5-fold at weaning (Table I), in line with previously reported changes of mRNA levels (40).

Of immense importance for the efficient uptake of intact immunoglobulins in the neonatal period is also the appearance of specialized apical endosomes. In suckling rodents, large endosomes at the base of the microvilli provide the efficient uptake of IgG-receptor complexes, which are then transported with vesicles across the cell for release by exocytosis at the basolateral cell surface. In addition, the large endosomes provide a low level of non-selective protein uptake, which directs proteins to lysosomes (41). Endocytic endosomes have been reported to appear in rats a few days before birth and persist through the suckling period (11). We identified apical endosomal glycoprotein, which is a marker for these specialized apical endosomes, and found a high expression during the suckling period and a 5.5-fold decline at weaning, *i.e.* consistent with the reported presence of endocytic endosomes in rats (Table I). To our knowledge, the expression of apical endosomal glycoprotein along intestinal development has not previously been reported and its function remains to be elucidated (42, 43). Our quantification of neonatal Fc receptor and the less characterized apical endosomal glycoprotein shed light onto the postnatal acquisition of passive immunity in mice. A possible future experimental setup using membrane-enriched fractions would enable to further explore immunological functions of the cells and their sensing of microbial signals, *for example,* by the temporal expression of common innate molecule receptors, such as toll-like receptors and collectins.

Other Biological Processes—The final common pathway in the metabolism of the main types of macronutrients (carbohydrates, lipids, and proteins) is the citric acid cycle. All enzymes of the citric acid cycle except pyruvate dehydrogenase were identified, including different subsets and isoforms of several of the enzymes (Fig. 4, supplemental Table S4). These results exemplify the extensiveness of the data set and the level of complexity of the citric acid cycle goes beyond the interpretation scope of this report. However, our results on the temporal expression patterns of different isoforms of several proteins as discussed above, including fatty acid binding proteins and isozymes involved in glycolysis, may contribute to a better understanding of the roles of the specific isoforms in the small intestine.

The processes of digestion and absorption of the small intestine require a continuous energy supply, *i.e.* ATP. In most cells the majority of ATP is generated in the mitochondrial electron transport chain. Proteins of the biological process of electron transport were found to have an overall trend of reduced expression after the first week of age, indicating a decline in energy-generating capacity in the small intestine (Fig. 4 and supplemental Table S4). Subunits of all four complexes of the mitochondrial electron transport chain were identified (NADH dehydrogenase, succinate dehydrogeanse, cytochrome b-c1 complex, and cytochrome *c* oxidase), as well as cytochrome *c* and ATP-synthase. A marked decrease (40-fold and 13-fold) was found in the middle suckling period for two subunits of NADH dehydrogenase (ubiquinone) 1 α. Further, one subunit of cytochrome *c* oxidase was decreased 25-fold from 7 D to 35 D. Similar age-related changes have been shown in duodenum of rats (44).

To our knowledge, temporal expression patterns of proteins implicated in cell structure have not been previously described in the context of intestinal development. We identified numerous such proteins and interestingly found subtle changes in expression during early suckling and more pronounced changes in the middle-suckling and weaning period (Fig. 4, supplemental Table S4). Proteins involved in microfilamentous structures, including villin, filamin, and spectrin, were found to be higher expressed along the maturation (Table I). Villin, which is known to specifically anchor to the core of actin filaments at the tip of microvilli of intestinal epithelial cells, showed a modest but continuous increase along the maturation. Filamin is known to be associated with the microfilaments in the terminal web (horizontal network of actin filaments lying just below the base of microvilli) and spectrin anchors the terminal web to the apical membrane of a cell. Both proteins showed a similar expression profile along maturation, with an increase during middle-suckling and weaning period. Although the structural changes and growth of the intestine starts already during gestation and continue in postnatal life until after weaning (8), our results suggest that morphological changes of the cells are minimal during the first week of age in mice and may be more physiologically important during middle-suckling and weaning to increase the capacity to digest and absorb nutrients. For example, major structural changes are known to occur during suckling and weaning as the presence of large endosomes gradually decreases (11, 45).

Conclusions—Based on quantitative proteomics of primary IECs, we have generated a unique and extensive data set of protein abundance changes that define *in vivo* intestinal development. We have illustrated a major change in function of the cells after the first postnatal week and by monitoring several biological processes, we have suggested that abundance changes of proteins involved in fatty acid metabolism and lactose metabolism are not driven by the diet itself. In addition, our data contribute to a better understanding of the roles of specific isoforms in the enterocytes of the small intestine. Independent protein-based assays may now be used to focus on target proteins for biomarker discovery and a similar study design using, for example, germ-free mice could give a better understanding of the role of microbiota in the development of the intestine. In conclusion, we have illustrated for the first time at proteome scale, a global and in-depth view on the temporal changes that occur in enterocytes to prepare for and adapt to the nutritional changes to optimize nutrient absorption during the postnatal development.

S This article contains supplemental Tables S1 to S4.

‖ To whom correspondence should be addressed: Functional Genomics Group, Vers-chez-les-Blanc, CH-1000 Lausanne 26. Phone: +41 21 785 82 25; Fax: +41 21 785 85 66; E-mail: jenny.hansson@rdls.nestle.com.

REFERENCES

1. Danielsen, M., Hornshøj, H., Siggers, R. H., Jensen, B. B., van Kessel, A. G., and Bendixen, E. (2007) Effects of bacterial colonization on the porcine intestinal proteome. *J. Proteome. Res.* **6,** 2596–2604
2. Greco, S., Hugueny, I., George, P., Perrin, P., Louisot, P., and Biol, M. C. (2000) Influence of spermine on intestinal maturation of the glycoprotein glycosylation process in neonatal rats. *Biochem. J.* **345 Pt 1,** 69–75
3. Hooper, L. V. (2004) Bacterial contributions to mammalian gut development. *Trends Microbiol.* **12,** 129–134
4. Rådberg, K., Biernat, M., Linderoth, A., Zabielski, R., Pierzynowski, S. G., and Weström, B. R. (2001) Enteral exposure to crude red kidney bean lectin induces maturation of the gut in suckling pigs. *J. Anim Sci.* **79,** 2669–2678
5. Strzalkowski, A. K., Godlewski, M. M., Hallay, N., Kulasek, G., Gajewski, Z., and Zabielski, R. (2007)The effect of supplementing sow with bioactive substances on neonatal small intestinal epithelium. *J. Physiol Pharmacol.* **58 Suppl 3**,115–122
6. de Santa Barbara, P., van den Brink, G. R., and Roberts, D. J. (2003) Development and differentiation of the intestinal epithelium. *Cell Mol. Life Sci.* **60,** 1322–1332
7. Cummins, A. G., Jones, B. J., and Thompson, F. M. (2006) Postnatal epithelial growth of the small intestine in the rat occurs by both crypt fission and crypt hyperplasia. *Dig. Dis. Sci.* **51,** 718–723
8. Buddington, R. K. (1994) Nutrition and ontogenetic development of the intestine. *Can. J. Physiol Pharmacol.* **72,** 251–259
9. Henning, S. J. (1981) Postnatal development: coordination of feeding, digestion, and metabolism. *Am. J. Physiol.* **241,** G199-G214
10. Moxey, P. C., and Trier, J. S. (1979) Development of villus absorptive cells in the human fetal small intestine: a morphological and morphometric study. *Anat. Rec.* **195,** 463–482
11. Kraehenbuhl, J. P., Bron, C., and Sordat, B. (1979) Transfer of humoral secretory and cellular immunity from mother to offspring. *Curr. Top. Pathol.* **66,** 105–157
12. Fanaro, S., Chierici, R., Guerrini, P., and Vigi, V. (2003) Intestinal microflora in early infancy: composition and development. *Acta Paediatr. Suppl* **91,** 48–55
13. Mackie, R. I., Sghir, A., and Gaskins, H. R. (1999) Developmental microbial ecology of the neonatal gastrointestinal tract. *Am. J. Clin. Nutr.* **69,** S1035- S1045
14. Neish, A. S. (2009) Microbes in gastrointestinal health and disease. *Gastroenterology* **136,** 65–80
15. Sekirov, I., Russell, S. L., Antunes, L. C., and Finlay, B. B. (2010) Gut microbiota in health and disease. *Physiol. Rev.* **90,** 859–904
16. Fang, R., Olds, L. C., and Sibley, E. (2006) Spatio-temporal patterns of intestine-specific transcription factor expression during postnatal mouse gut development. *Gene Expr. Patterns.* **6,** 426–432
17. Gordon, J. I., Elshourbagy, N., Lowe, J. B., Liao, W. S., Alpers, D. H., and Taylor, J. M. (1985) Tissue specific expression and developmental regulation of two genes coding for rat fatty acid binding proteins. *J. Biol. Chem.* **260,** 1995–1998
18. Jenkins, S. L., Wang, J., Vazir, M., Vela, J., Sahagun, O., Gabbay, P., Hoang, L., Diaz, R. L., Aranda, R., and Martín, M. G. (2003) Role of passive and adaptive immunity in influencing enterocyte-specific gene expression. *Am. J. Physiol. Gastrointest. Liver Physiol* **285,** G714–G725
19. Lu, S., Huffman, M., Yao, Y., Mansbach, C. M., 2nd, Cheng, X., Meng, S., and Black, D. D. (2002) Regulation of MTP expression in developing swine. *J. Lipid Res.* **43,** 1303–1311
20. Mochizuki, K., Mochizuki, H., Kawai, H., Ogura, Y., Shimada, M., Takase, S., and Goda, T. (2007) Possible role of fatty acids in milk as the regulator of the expression of cytosolic binding proteins for fatty acids and vitamin A through PPARalpha in developing rats. *J. Nutr. Sci. Vitaminol.* **53,** 515–521
21. Mochizuki, K., Yorita, S., and Goda, T. (2009) Gene expression changes in the jejunum of rats during the transient suckling-weaning period. *J. Nutr. Sci. Vitaminol.* **55,** 139–148
22. deSchoolmeester, M. L., Manku, H., and Else, K. J. (2006) The innate immune responses of colonic epithelial cells to Trichuris muris are similar in mouse strains that develop a type 1 or type 2 adaptive immune response. *Infect. Immun.* **74,** 6280–6286
23. Zhou, P., Streutker, C., Borojevic, R., Wang, Y., and Croitoru, K. (2004) IL-10 modulates intestinal damage and epithelial cell apoptosis in T cell-mediated enteropathy. *Am. J. Physiol. Gastrointest. Liver Physiol* **287,** G599-G604
24. Al-Shahrour, F., Minguez, P., Tárraga, J., Montaner, D., Alloza, E., Vaquerizas, J. M., Conde, L., Blaschke, C., Vera, J., and Dopazo, J. (2006) BABELOMICS: a systems biology perspective in the functional annotation of genome-scale experiments. *Nucleic Acids Res.* **34,** W472–W476
25. Thomas, P. D., Campbell, M. J., Kejariwal, A., Mi, H., Karlak, B., Daverman, R., Diemer, K., Muruganujan, A., and Narechania, A. (2003) PANTHER: a library of protein families and subfamilies indexed by function. *Genome Res.* **13,** 2129–2141
26. Dennis, G., Jr., Sherman, B. T., Hosack, D. A., Yang, J., Gao, W., Lane, H. C., and Lempicki, R. A. (2003) DAVID: Database for annotation, visualization, and integrated discovery. *Genome Biol.* **4,** 3
27. Huang da, W., Sherman, B. T., and Lempicki, R. A. (2009) Systematic and integrative analysis of large gene lists using DAVID bioinformatics resources. *Nat. Protoc.* **4,** 44–57
28. Chang, J., Chance, M. R., Nicholas, C., Ahmed, N., Guilmeau, S., Flandez, M., Wang, D., Byun, D. S., Nasser, S., Albanese, J. M., Corner, G. A., Heerdt, B. G., Wilson, A. J., Augenlicht, L. H., and Mariadason, J. M. (2008) Proteomic changes during intestinal cell maturation in vivo. *J. Proteomics.* **71,** 530–546
29. Weber, G. (1983) Biochemical strategy of cancer cells and the design of chemotherapy: G. H. A. Clowes Memorial Lecture. *Cancer Res.* **43,** 3466–3492
30. Rautava, S., and Walker, W. A. (2007) Commensal bacteria and epithelial cross talk in the developing intestine. *Curr. Gastroenterol. Rep.* **9,** 385–392
31. Kent, J. C. (2007) How breastfeeding works. *J. Midwifery Womens Health* **52,** 564–570
32. Gygi, S. P., Rochon, Y., Franza, B. R., and Aebersold, R. (1999) Correlation between protein and mRNA abundance in yeast. *Mol. Cell. Biol.* **19,** 1720–1730
33. Nie, L., Wu, G., Culley, D. E., Scholten, J. C., and Zhang, W. (2007) Integrative analysis of transcriptomic and proteomic data: challenges, solutions and applications. *Crit Rev. Biotechnol.* **27,** 63–75
34. Tso, P., Nauli, A., and Lo, C. M. (2004) Enterocyte fatty acid uptake and intestinal fatty acid-binding protein. *Biochem. Soc. Trans.* **32,** 75–78
35. Stahl, A., Hirsch, D. J., Gimeno, R. E., Punreddy, S., Ge, P., Watson, N., Patel, S., Kotler, M., Raimondi, A., Tartaglia, L. A., and Lodish, H. F. (1999) Identification of the major intestinal fatty acid transport protein. *Mol. Cell* **4,** 299–308
36. Cao, J., Hawkins, E., Brozinick, J., Liu, X., Zhang, H., Burn, P., and Shi, Y. (2004) A predominant role of acyl-CoA:monoacylglycerol acyltransferase-2 in dietary fat absorption implicated by tissue distribution, subcellular localization, and up-regulation by high fat diet. *J. Biol. Chem.* **279,** 18878–18886
37. Coleman, R. A., and Haynes, E. B. (1984) Hepatic monoacylglycerol acyltransferase. Characterization of an activity associated with the suckling period in rats. *J. Biol. Chem.* **259,** 8934–8938
38. Danielsen, M., Thymann, T., Jensen, B. B., Jensen, O. N., Sangild, P. T., and Bendixen, E. (2006) Proteome profiles of mucosal immunoglobulin uptake in inflamed porcine gut. *Proteomics.* **6,** 6588–6596
39. Rodewald, R. (1980) Distribution of immunoglobulin G receptors in the small intestine of the young rat. *J. Cell Biol.* **85,** 18–32
40. Gill, R. K., Mahmood, S., Sodhi, C. P., Nagpaul, J. P., and Mahmood, A. (1999) IgG binding and expression of its receptor in rat intestine during postnatal development. *Indian J. Biochem. Biophys.* **36,** 252–257
41. Abrahamson, D. R., and Rodewald, R. (1981) Evidence for the sorting of endocytic vesicle contents during the receptor-mediated transport of IgG across the newborn rat intestine. *J. Cell Biol.* **91,** 270–280
42. Allen, K., Gokay, K. E., Thomas, M. A., Speelman, B. A., and Wilson, J. M. (1998) Biosynthesis of endotubin: an apical early endosomal glycoprotein from developing rat intestinal epithelial cells. *Biochem. J.* **330 (Pt 1),** 367–373
43. McCarter, S. D., Johnson, D. L., Kitt, K. N., Donohue, C., Adams, A., and Wilson, J. M. (2010) Regulation of tight junction assembly and epithelial polarity by a resident protein of apical endosomes. *Traffic.* **11,** 856–866
44. Lee, H. M., Greeley, G. H., Jr., and Englander, E. W. (2001) Age-associated changes in gene expression patterns in the duodenum and colon of rats. *Mech. Ageing Dev.* **122,** 355–371
45. Skrzypek, T., Valverde Piedra, J. L., Skrzypek, H., Kazimierczak, W., Biernat, M., and Zabielski, R. (2007)Gradual disappearance of vacuolated enterocytes in the small intestine of neonatal piglets. *J. Physiol Pharmacol.* **58 Suppl 3,** 87–95